Development of in situ two-coil mutual inductance technique in a multifunctional scanning tunneling microscope

Ming-Chao Duan, Zhi-Long Liu, Jian-Feng Ge, Zhi-Jun Tang, Guan-Yong Wang, Zi-Xin Wang, Dandan Guan, Yao-Yi Li, Dong Qian, Canhua Liu, and Jin-Feng Jia

Citation: Review of Scientific Instruments **88**, 073902 (2017); doi: 10.1063/1.4991819
View online: http://dx.doi.org/10.1063/1.4991819
View Table of Contents: http://aip.scitation.org/toc/rsi/88/7
Published by the American Institute of Physics

Development of *in situ* two-coil mutual inductance technique in a multifunctional scanning tunneling microscope

Ming-Chao Duan,[1] Zhi-Long Liu,[1] Jian-Feng Ge,[1] Zhi-Jun Tang,[1] Guan-Yong Wang,[1] Zi-Xin Wang,[2] Dandan Guan,[1,3] Yao-Yi Li,[1,3] Dong Qian,[1,3] Canhua Liu,[1,3,a)] and Jin-Feng Jia[1,3,a)]

[1]*Key Laboratory of Artificial Structures and Quantum Control (Ministry of Education), School of Physics and Astronomy, Shanghai Jiao Tong University, 800 Dongchuan Road, Shanghai 200240, China*
[2]*School of Electronics and Information Technology, Sun Yat-Sen University, 135 Xingang Xi Road, Guangzhou 510275, China*
[3]*Collaborative Innovation Center of Advanced Microstructures, Nanjing 210093, China*

(Received 13 February 2017; accepted 19 June 2017; published online 10 July 2017)

Superconducting thin films have been a focal point for intensive research efforts since their reduced dimension allows for a wide variety of quantum phenomena. Many of these films, fabricated in UHV chambers, are highly vulnerable to air exposure, making it difficult to measure intrinsic superconducting properties such as zero resistance and perfect diamagnetism with *ex situ* experimental techniques. Previously, we developed a multifunctional scanning tunneling microscope (MSTM) containing *in situ* four-point probe (4PP) electrical transport measurement capability in addition to the usual STM capabilities [Ge *et al.*, Rev. Sci. Instrum. **86**, 053903 (2015)]. Here we improve this MSTM via development of both transmission and reflection two-coil mutual inductance techniques for *in situ* measurement of the diamagnetic response of a superconductor. This addition does not alter the original STM and 4PP functions of the MSTM. We demonstrate the performance of the two-coil mutual inductance setup on a 10-nm-thick NbN thin film grown on a Nb-doped $SrTiO_3(111)$ substrate. *Published by AIP Publishing.* [http://dx.doi.org/10.1063/1.4991819]

I. INTRODUCTION

Two-coil mutual inductance techniques have been used to study two-dimensional (2D) superconductivity by detecting diamagnetic properties in a wide range of 2D superconductors including the Kosterlitz-Thouless transition in thin aluminum films,[1] the proximity-effect in a 2D-array of Josephson junctions,[2] and the penetration depth in epitaxial NbN thin films.[3] Very recently, these techniques have also been applied to investigate the superfluid density of the thin film copper oxide superconductor $La_{2-x}Sr_xCuO_4$.[4] To the best of our knowledge, previously reported experiments using this technique were all performed in *ex situ* conditions, which are not suitable for materials that are vulnerable to air such as Pb and In atomic layers on Si surfaces[5–7] or K doped FeSe films.[8–13] One solution to this problem is to use protective layers to cover the sample surface. This method was applied to a two-coil inductance measurement of single-layer FeSe grown on a $SrTiO_3$ substrate[14,15] on top of which multiple capping layers were carefully fabricated.[16,17] An alternative solution is to perform *in situ* two-coil mutual inductance measurements, which could effectively protect samples from damage via atmosphere or improper protection layers.

In this report, we have developed a two-coil mutual inductance setup based on a multifunctional scanning tunneling microscope (MSTM) that is capable of not only the usual STM functionality but also *in situ* four-point probe (4PP) electrical transport measurements owing to a self-designed 4-electrode piezo-scanner tube.[18] With this additional development, the systematic study of a superconducting film can be performed by measuring electrical and diamagnetic properties at varied temperatures (≥320 mK) and in high magnetic fields (≤11 T) all within a single UHV chamber. This enables experimental data to be collected more efficiently and analyzed in a more credible way since it can all be taken for one sample without the risk of damage.

II. INSTRUMENT DEVELOPMENT

A transmission-type two-coil mutual inductance technique typically consists of two coaxial coils placed on two sides of a sample, as shown schematically in Fig. 1(a). An alternating magnetic field [indicated by yellow arrows in Fig. 1(a)] is induced by an alternating current applied to the drive coil. This in turn generates an alternating voltage in the pickup coil, which reflects the mutual inductance of the two coils and can be measured with a lock-in amplifier. When a superconducting sample is placed between the drive and pickup coils it will in principle shield the induced magnetic field and cause a reduction in the generated voltage, as illustrated schematically by blue arrows in Fig. 1(a).

Figure 1(b) shows the schematic of a reflection-type two-coil mutual inductance setup, in which both drive and pickup coils are coaxially placed on one side of a sample. To increase sensitivity, the pickup coil is formed into a differential coil, i.e., a pair of counter-wound coils with the same geometry which are connected in series and put symmetrically on two sides

a)Authors to whom correspondence should be addressed: canhualiu@sjtu.edu.cn and jfjia@sjtu.edu.cn

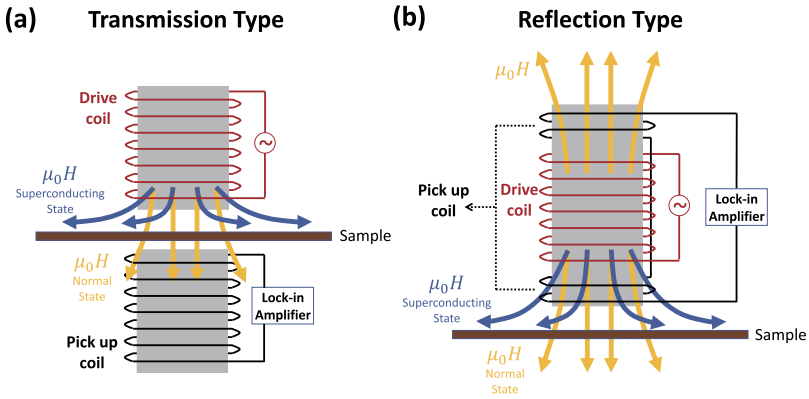

FIG. 1. Schematic illustration of the two-coil mutual inductance measurement in (a) transmission-type and (b) reflection-type configurations. Yellow and blue arrows denote the magnetic flux lines emitted from the drive coil when the sample is in the normal and superconducting states, respectively.

of the drive coil. When the sample is in its normal state, the induced voltages in the pair of counter-wound coils are equal (or almost equal due to their imperfect similarity) but opposite in sign, resulting in a net output of (nearly) zero voltage in the pickup coil. In the superconducting state of the sample, the balance between the two pickup coils is destroyed due to the significant shielding of the magnetic field on only one side of the coils. This results in a net increase in the total output voltage for the pickup coil.

The *in situ* two-coil mutual inductance setup we have developed is based on a self-designed MSTM[18] consisting of an Molecular Beam Epitaxy (MBE) system and an STM system (from UNISOKU, Co.) that can be operated at low temperatures (≥320 mK) and in high magnetic fields (≤11 T). The MSTM differs from a conventional STM in that it contains a piezo-scanner tube with four earphone-socket-like electrodes, as shown schematically in Fig. 2(a). The 4PP is installed on a probe holder with four earphone-plug-like electrodes [Fig. 2(b)] to match the shape of the scanner tube. This shaping is crucial as it allows the STM and 4PP measurements to be freely interchangeable within the same sample mount.

Figure 2(c) shows the schematic for a sample holder with a mounted sample wafer with a reflection-type two-coil mutual inductance setup mounted below it on the custom probe holder for our MSTM. The drive coil (red) and differential pickup coil (black) are coaxially wound on a 1.6 mm diameter 8.0 mm long ceramic rod (gray) and made from 25-μm-diameter enameled gold wires. The drive coil has 300 turns extending ~1.0 mm along the ceramic rod. Each of the two mutually compensating sections of the pickup coil has 10 turns extending only ~0.1 mm along the rod and they are separated from the two ends of the drive coil by ~0.3 mm. All coil wires are electrically connected to four metal poles on the probe holder using conductive adhesive. Figure 2(d) shows a photo of the reflection-type two-coil mutual inductance setup in which the ceramic rod with coils is fixed by insulating cement and is standing on the probe holder.

Figure 2(e) shows the schematic for a transmission-type mutual inductance setup. The drive coil has 400 turns of 50-μm-diameter enameled copper wire on a ceramic spool with a diameter of 1.0 mm and a length of 5 mm. The ceramic spool is fixed and standing on the sample holder side, where there are six electrodes available (not seen in the schematic, made by UNISOKU, Co.): two of them apply current to the drive coil and the other two are used for current heating of the sample. The coil wires are covered by an insulating paste that is vulnerable to heat, so a gap of ~1 mm is left between the top of the coil and the sample wafer where heat is applied to regulate the temperature. We found that the drive coil operated correctly even after the sample wafer had been kept at ~900 °C for 2 h. A photo of the sample holder containing a drive coil is shown in Fig. 2(f), where the sample wafer is replaced by a transparent green square for a better view of the drive coil.

The pickup coil of the transmission-type mutual inductance has 20 turns of 25-μm-diameter enameled gold wire on a ceramic spool with a diameter of 0.2 mm and a length of 0.8 mm. The spool is fixed on a thicker ceramic tube with an inner diameter of 0.2 mm, an outer diameter of 2 mm, and a length of 5 mm. The ceramic tube is then fixed and standing on the probe holder in a similar setup to that of the

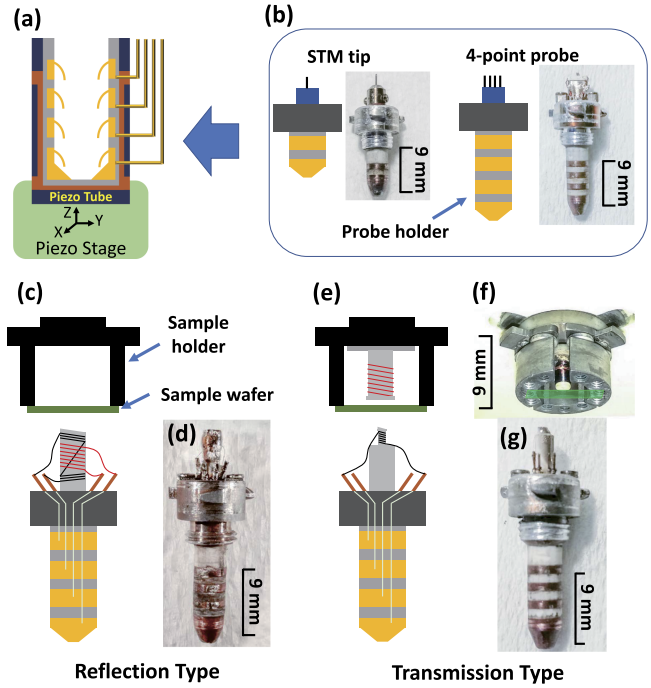

FIG. 2. Illustration of the experimental setup. (a) Schematic of the self-designed piezo-scanner tube with 4 earphone-socket-like electrodes. (b) Schematics and photos of STM tip and 4-point probe. [(c) and (e)] Schematics of the reflection- and transmission-type two-coil mutual inductance measurement setups, respectively. [(d) and (g)] Photos of the reflection- and transmission-type coil probes, respectively. (f) Photo of the sample holder containing the transmission-type drive coil.

reflection-type mentioned above. Figure 2(g) shows the photo of the transmission-type pickup coil.

To improve sensitivity of the mutual inductance measurement, the pickup coil needs to be placed as close as possible to the sample wafer. In practice, the probe holder is driven by the STM piezo slider until its top touches sample surface, where the mutual inductance stops changing. The rod top is slightly beveled so that the contact area with the sample surface is reduced as much as possible to minimize damage to the sample surface. In practice, the contact is gentle enough that hardly any scuffing was observed on the sample surface under an optical microscope after several mutual inductance measurements were taken for ultrathin films grown on Si(111) or $SrTiO_3$(001) surfaces.

The circuit for the mutual inductance measurement is demonstrated schematically in Fig. 3(a). The drive and pickup coils are electrically connected to a Keithley 6221 sourcemeter and an OE1022 DSP lock-in amplifier (from Innovative Laboratory of SYSU) using coaxial shielded cables. The overall noise level of the measurement system is below 10 nV. A Lakeshore 350 controller is used to change the sample temperature by adjusting the output power to a heater near the sample stage, and a Cryogenic SMS 100 controller is used to generate magnetic fields perpendicular to the sample surface up to 11 T. The devices and controllers are remotely controlled by self-developed programs written in LabView 2011. Parameter input, data acquisition, temperature control, and magnetic field control are all integrated into the main program. Measurement proceeds automatically after the parameters are set properly.

Figure 3(b) shows the equivalent circuit for the mutual inductance measurement setup. A load resistance R of 10 kΩ is connected in series with the drive coil to stabilize the phase of excitation currents less than 200 μA. M represents the mutual inductance between the drive and pickup coils. R_d and R_p represent the resistance of the drive and that of the pickup coils, respectively. They are about 20 Ω (40 Ω) and 5 Ω (7 Ω) in the transmission (reflection) type setup at room temperature, respectively. The voltage applied to drive coil is also sent as an input to the lock-in amplifier to act as an external reference signal. The desired phase difference between the output of the pickup coil and the reference signal is 90°. Due to a parasitic capacitance C between the drive and pickup coils,[19] however, a spurious phase shift occurs and the actual phase difference is measured to be 90° ± 5°.

III. PERFORMANCES

To demonstrate the performance of the mutual inductance measurement system, a NbN film with a thickness of about 10 nm grown on a Nb-doped $SrTiO_3$(111) substrate was used. NbN is a well-known conventional superconductor with a bulk critical temperature (T_c) of about 16 K.[20] However, its critical temperature is highly sensitive to sample thickness for thin films.[21]

The NbN thin film was epitaxially grown in another UHV chamber equipped with a commercial STM. One typical STM image taken just after the sample growth is shown in Fig. 4(a), where flat terraces and sharp steps are visible. The NbN film was installed in our UHV chamber after a month of exposure to air, which contaminated the film surface and thus made STM observations nearly impossible even after considerable outgassing had been carried out. However, a dI/dV tunneling spectrum showing a superconducting energy gap was easily collected at an arbitrary location on the sample, as shown in Fig. 4(b), indicating that the contaminations on the surface did not destroy the superconductivity of the NbN film. After subtracting a polynomial background, the typical dI/dV spectrum can be well fitted to a Dynes function[22] with an appropriate quasiparticle-lifetime broadening factor.[23] The gap is found to be 1.66 meV, which is consistent with a previous report.[3]

The two-coil mutual inductance measurement on the NbN thin film was carried out after *in situ* exchange of the coil and STM probe holders. In both transmission- and reflection-type measurements, the NbN film sample was first cooled down to 7.8 K, which is the lowest accessible temperature in the instrument without using a thermo-shielding cap or a He^3 cooling system. The sample temperature was then increased under Proportion Integration Differentiation (P.I.D.) control in intervals of 0.5 K every 30 s [for data in Fig. 5(a)] or 0.25 K every 15 s [for data in Fig. 5(b)]. At each temperature step, the output bias of the pickup coil V_P was taken to be the mean value of 10 data points measured over 10 s. During the entire measurement process, an alternating current with an amplitude of 1414 μA (60 μA) and a frequency of 9991 Hz was applied through

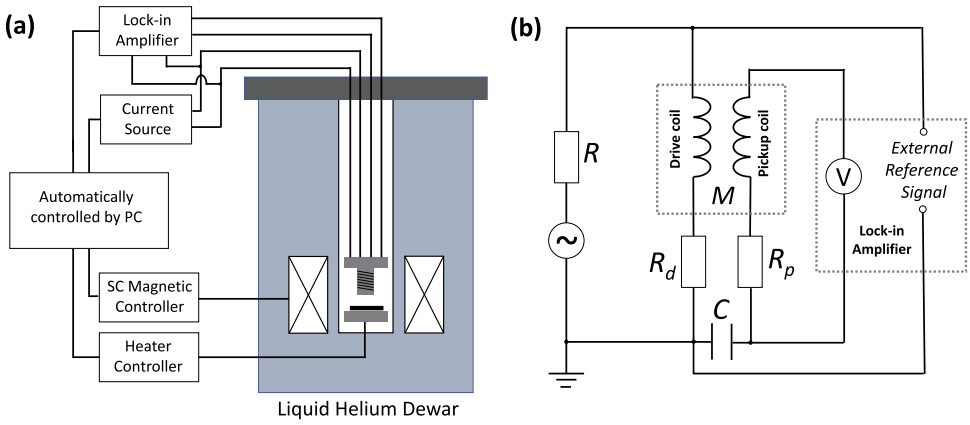

FIG. 3. Schematic illustration of the circuit for the two-coil mutual inductance measurement setup. (a) General circuit diagram consisting of control devices and the experimental environment. Boxed components are electrical devices denoted by their names. (b) Equivalent circuit of the mutual inductance measurement setup. The mutual inductor M represents the coupling between the drive and pickup coils. The dotted box on the right denotes a lock-in amplifier that measures voltages from both the pickup coil and a reference signal from the current source.

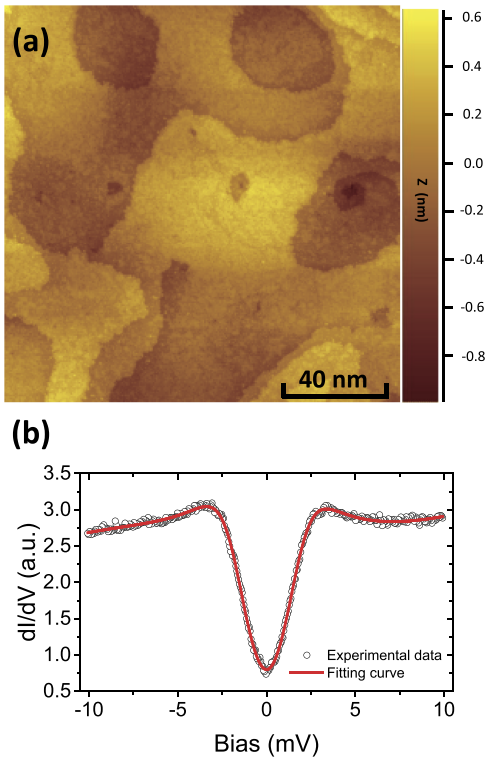

FIG. 4. (a) A typical STM image of the 10-nm-thick NbN film (V_{bias} = 1 V, I_t = 0.1 nA). (b) A tunneling spectrum of the NbN thin film taken at 7.8 K. The black hollow circles represent experimental data. The amplitude and frequency of bias modulation are 100 μV and 987 Hz, respectively. The red line is the fitting result.

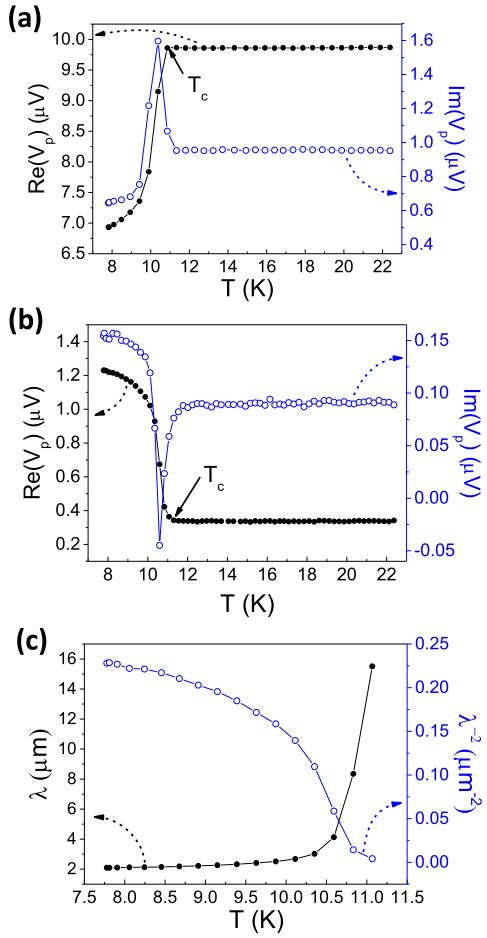

FIG. 5. Mutual inductance measurement results from (a) transmission-type and (b) reflection-type configurations. (c) Magnetic penetration depth λ and superfluid density $n_s \propto \lambda^{-2}$ extracted from the reflection-type measurement results. The curved arrows indicate the Y axis location corresponding to each data set.

the transmission-type (reflection-type) drive coil generating a magnetic field at the sample surface less than 10^{-4} T, which is less than the lower critical magnetic field (4×10^{-3} T) of a NbN film reported in a previous study, and no signs of approaching the sample's critical field were observed.[24]

The measured V_p as a function of temperature in the transmission- and reflection-type configurations is shown in Figs. 5(a) and 5(b), respectively. Both reveal a remarkable superconducting transition at $T_c \sim 11$ K indicated by the real component of the V_p(T) curves. In the imaginary part of each V_p(T) curve, the peak (transmission-type) or dip (reflection-type) may relate to energy dissipation due to the vortex-antivortex unbinding mechanism that had been suggested in previous studies.[1,2] This is not a surprising result since the existence of a Kosterlitz-Thouless transition in a NbN film has been previously reported.[21]

From the reflection-type measurement results shown in Fig. 5(b), one can extract the magnetic penetration depth λ and the superfluid density $n_s \propto \lambda^{-2}$. The difference of V_p at a temperature lower than T_c from that at T_c satisfies the following equation:[25,26]

$$\delta V_p = \Delta Re\left(V_p\right) - i\Delta Im\left(V_p\right) = \omega I \int_0^\infty dx \frac{M(x)}{1 + (2/\mu_0 h)(1/i\omega G)x}, \quad (1)$$

where ω and I are angular frequency and amplitude of the driven current, respectively, μ_0 is the permeability of vacuum, and h is a sum of the distance from the drive and pickup coils to the sample. $M(x)$ is a geometrical factor expressed as

$$M(x) = \pi\mu_0\left(\frac{R_d R_p}{h}\right) J_1(R_d x/h) J_1(R_p x/h) e^{-x} \times \frac{(1 - e^{-l_d x/h})(1 - e^{-l_p x/h})}{(1 - e^{-l_d x/(hN_d)})(1 - e^{-l_p x/(hN_p)})}, \quad (2)$$

where R_d, R_p, l_d, l_p, N_d, and N_p are radii, lengths, and turns of the drive and pickup coils, respectively. J_1 is the first-order Bessel function. By numerically solving Eq. (1), one can obtain the complex ac conductivity G, which is related to the penetration depth λ and thickness of the film d via the following equations:

$$G = \frac{1}{R + i\omega L}, \quad (3)$$

$$L = \mu_0 \lambda \coth\left(\frac{d}{\lambda}\right). \quad (4)$$

Figure 5(c) displays the extracted λ and corresponding λ^{-2} as a function of temperature, both of which have very similar curve shapes with those in previous reports.[3,21] It is noted that the data analysis above is based on a model that assumes the size of the film is infinite. In our experimental setup, however, the in-plane size of the sample film is 2×8 mm^2, which is comparable to that of the reflection-type

pickup coil (diameter is 1.6 mm). Therefore the values for λ obtained here are expected to be significantly larger than the intrinsic ones. In fact, the estimates for λ obtained here are an order of magnitude larger than those in the literature.[3,21]

IV. CONCLUSION

We developed a two-coil mutual inductance measurement setup based on a self-designed MSTM that has four electrodes on its piezo-scanner tube. This MSTM enables *in situ* measurement of the diamagnetic response of a superconducting thin film as well as STM and 4PP electrical transport measurements. The performance of the two-coil mutual inductance measurement is validated by experiments on a 10-nm-thick NbN film grown on a Nb-doped $SrTiO_3$ substrate, which exhibits a distinct superconducting transition at 11 K. This setup is a reliable tool for the systematic investigation of intrinsic superconductivity in novel low-dimensional materials. It has been recently applied to study ultrathin superconducting films including the Si(111)-$\sqrt{7} \times \sqrt{3}$-In superstructure and K doped 2-triple-layer FeSe films grown on a $SrTiO_3$(001) substrate.

ACKNOWLEDGMENTS

Financial support from the National Basic Research Program of China (Grant Nos. 2016YFA0300403, 2016YFA0301003, and 2013CB921902), NSFC (Grant Nos. 11574202, 11521404, 11634009, 91421312, U1632272, 11574201, 11504230, and U1632102), and Shanghai Committee of Science and Technology, China (Grant Nos. 15JC402300 and 14XD1401900) is appreciated. C.L. and D.Q. acknowledge support from the Changjiang Scholars Program. C.L. also acknowledges support from the Shuguang Program of Shanghai Education Development Foundation and Shanghai Municipal Education Commission.

[1] A. F. Hebard and A. T. Fiory, Phys. Rev. Lett. **44**, 291 (1980).
[2] C. Leemann, P. Lerch, G. Racine, and P. Martinoli, Phys. Rev. Lett. **56**, 1291 (1986).
[3] A. Kamlapure, M. Mondal, M. Chand, A. Mishra, J. Jesudasan, V. Bagwe, L. Benfatto, V. Tripathi, and P. Raychaudhuri, Appl. Phys. Lett. **96**, 072509 (2010).
[4] I. Bozovic, X. He, J. Wu, and A. T. Bollinger, Nature **536**, 309 (2016).
[5] T. Zhang, P. Cheng, W.-J. Li, Y.-J. Sun, G. Wang, X.-G. Zhu, K. He, L. Wang, X. Ma, X. Chen, Y. Wang, Y. Liu, H.-Q. Lin, J.-F. Jia, and Q.-K. Xue, Nat. Phys. **6**, 104 (2010).
[6] M. Yamada, T. Hirahara, and S. Hasegawa, Phys. Rev. Lett. **110**, 237001 (2013).
[7] T. Uchihashi, P. Mishra, M. Aono, and T. Nakayama, Phys. Rev. Lett. **107**, 207001 (2011).
[8] C.-L. Song, H.-M. Zhang, Y. Zhong, X.-P. Hu, S.-H. Ji, L. Wang, K. He, X.-C. Ma, and Q.-K. Xue, Phys. Rev. Lett. **116**, 157001 (2016).
[9] Y. Miyata, K. Nakayama, K. Sugawara, T. Sato, and T. Takahashi, Nat. Mater. **14**, 775 (2015).
[10] W. H. Zhang, X. Liu, C. H. P. Wen, R. Peng, S. Y. Tan, B. P. Xie, T. Zhang, and D. L. Feng, Nano Lett. **16**, 1969 (2016).
[11] C. Tang, D. Zhang, Y. Zang, C. Liu, G. Zhou, Z. Li, C. Zheng, X. Hu, C. Song, S. Ji, K. He, X. Chen, L. Wang, X. Ma, and Q.-K. Xue, Phys. Rev. B **92**, 180507 (2015).
[12] C. Tang, C. Liu, G. Zhou, F. Li, H. Ding, Z. Li, D. Zhang, Z. Li, C. Song, S. Ji, K. He, L. Wang, X. Ma, and Q.-K. Xue, Phys. Rev. B **93**, 020507 (2016).
[13] C. H. Wen, H. C. Xu, C. Chen, Z. C. Huang, X. Lou, Y. J. Pu, Q. Song, B. P. Xie, M. Abdel-Hafiez, D. A. Chareev, A. N. Vasiliev, R. Peng, and D. L. Feng, Nat. Commun. **7**, 10840 (2016).
[14] Q.-Y. Wang, Z. Li, W.-H. Zhang, Z.-C. Zhang, J.-S. Zhang, W. Li, H. Ding, Y.-B. Ou, P. Deng, K. Chang, J. Wen, C.-L. Song, K. He, J.-F. Jia, S.-H. Ji, Y.-Y. Wang, L.-L. Wang, X. Chen, X.-C. Ma, and Q.-K. Xue, Chin. Phys. Lett. **29**, 037402 (2012).
[15] J. F. Ge, Z. L. Liu, C. Liu, C. L. Gao, D. Qian, Q. K. Xue, Y. Liu, and J. F. Jia, Nat. Mater. **14**, 285 (2015).
[16] W.-H. Zhang, Y. Sun, J.-S. Zhang, F.-S. Li, M.-H. Guo, Y.-F. Zhao, H.-M. Zhang, J.-P. Peng, Y. Xing, H.-C. Wang, T. Fujita, A. Hirata, Z. Li, H. Ding, C.-J. Tang, M. Wang, Q.-Y. Wang, K. He, S.-H. Ji, X. Chen, J.-F. Wang, Z.-C. Xia, L. Li, Y.-Y. Wang, J. Wang, L.-L. Wang, M.-W. Chen, Q.-K. Xue, and X.-C. Ma, Chin. Phys. Lett. **31**, 017401 (2014).
[17] Z. Zhang, Y.-H. Wang, Q. Song, C. Liu, R. Peng, K. A. Moler, D. Feng, and Y. Wang, Sci. Bull. **60**, 1301 (2015).
[18] J. F. Ge, Z. L. Liu, C. L. Gao, D. Qian, C. Liu, and J. F. Jia, Rev. Sci. Instrum. **86**, 053903 (2015).
[19] S. J. Turneaure, A. A. Pesetski, and T. R. Lemberger, J. Appl. Phys. **83**, 4334 (1998).
[20] S. P. Chockalingam, M. Chand, J. Jesudasan, V. Tripathi, and P. Raychaudhuri, Phys. Rev. B **77**, 214503 (2008).
[21] J. Yong, T. R. Lemberger, L. Benfatto, K. Ilin, and M. Siegel, Phys. Rev. B **87**, 184505 (2013).
[22] T. Nishio, M. Ono, T. Eguchi, H. Sakata, and Y. Hasegawa, Appl. Phys. Lett. **88**, 113115 (2006).
[23] R. C. Dynes, V. Narayanamurti, and J. P. Garno, Phys. Rev. Lett. **41**, 1509 (1978).
[24] M. P. Mathur, D. W. Deis, and J. R. Gavaler, J. Appl. Phys. **43**, 3158 (1972).
[25] B. Jeanneret, J. L. Gavilano, G. A. Racine, C. Leemann, and P. Martinoli, Appl. Phys. Lett. **55**, 2336 (1989).
[26] Z. H. Lin, G. C. Spalding, A. M. Goldman, B. F. Bayman, and O. T. Valls, Europhys. Lett. **32**, 573 (1995).